Lab on a Chip

Cite this: *Lab Chip*, 2011, **11**, 2630

www.rsc.org/loc

TECHNICAL NOTE

Magnetic micropillars as a tool to govern substrate deformations†

Jimmy le Digabel,[a] Nicolas Biais,[b] Jérome Fresnais,[c] Jean-François Berret,[a] Pascal Hersen[a] and Benoit Ladoux*[a]

Received 29th March 2011, Accepted 11th May 2011
DOI: 10.1039/c1lc20263d

Magnetic actuated microdevices can be used to achieve several complex functions in microfluidics and microfabricated devices. For example, magnetic mixers and magnetic actuators have been proposed to help handling fluids at a small scale. Here, we present a strategy to create magnetically actuated micropillar arrays. We combined microfabrication techniques and the dispersion of magnetic aggregates embedded inside polymeric matrices to design micrometre scale magnetic features. By creating a magnetic field gradient in the vicinity of the substrate, well-defined forces were applied on these magnetic aggregates which in turn induced a deflection of the micropillars. By dispersing either spherical aggregates or magnetic nanowires into the gels, we can induce synchronized motions of a group of pillars or the movement of isolated pillars under a magnetic field gradient. When combined with microfabrication processes, this versatile tool leads to local as well as global substrate actuations within a range of dimensions that are relevant for microfluidics and biological applications.

Introduction

The potential applications of polymeric micro- and nano-structured materials to create devices are numerous and were widely studied in the past two decades.[1] In most cases, these structured substrates are constitutively passive to external stimuli. Recently, the design of actuable microstructured materials has become an important challenge with numerous potential applications.[2] For instance, the manipulation of fluids in microfluidic systems, to ensure transport and mixing, is still an unsolved problem and may be improved by adding several local actuators. Incorporating magnetic materials inside the raw polymeric material is an interesting alternative way to obtain active microfabricated structures.[3] Magnetic materials such as ferrofluids or magnetically doped PDMS have been used as valves.[2] However it remains a challenge to fabricate magnetic microstructures at the micrometre scale. Interestingly such actuable microscale substrates could also be used to study the role of physical forces in cell biology.[4] As living cells are constantly subjected to external forces, different *in vitro* manipulation techniques have been used to explore the cell response to external mechanical stimulations.[5] Again, these techniques suffer from different limitations either in the range of accessible forces, the position of the force transducer relative to the cell or the quantification of the applied forces. To overcome these limitations, micro- or nanometre-sized actuable features inserted within substrates compatible with cell culture and microfluidics are desirable. This will permit to exert well-characterized forces and will be an alternative to the aforementioned techniques.

Micropillar substrate is indeed a versatile tool that has been used for surface chemistry studies in the context of superhydrophobic substrates,[6] as multiple force sensors for cell mechanics[7–9] as well as topographical cues to study cell responses[10,11] and for controlling biomolecular interactions.[12] Such studies are based on the deposition of either liquid droplets or living cells on these micro-textured surfaces followed by wettability analysis or force measurements. In both cases, micropillars act as passive sensors. In this context, the micropillar substrate appears to be a great starting point for the design of actuated micro-substrates.

There have been many attempts to produce magnetic microfabricated devices.[3,13] However the insertion of magnetic particles inside polydimethylsiloxane (PDMS) elastomers, commonly used in soft lithography, leads to particle aggregation which makes them difficult to insert into microscale structures. Attempts to chemically modify magnetic particles[14] to help their dispersal in PDMS have yet to yield high enough particle density. Here we present a new strategy that is based on the incorporation of magnetic nanoparticles into hydrogels of various stiffnesses to fabricate magnetic microstructures. Making use of soft lithography techniques, we dispersed magnetic nanoparticles, either nanowires or magnetite nanoparticle complexes, into polyacrylamide (PAM)

[a]*Laboratoire Matière et Systèmes Complexes (MSC), Université Paris-Diderot & CNRS UMR 7057, Bâtiment Condorcet, Paris, France. E-mail: benoit.ladoux@univ-paris-diderot.fr; Fax: +33 (0)1 57 27 62 11; Tel: +33 (0)1 57 27 70 35*
[b]*Department of Biological Sciences, Columbia University, 1212 Amsterdam Ave., New York, NY, 11027, USA*
[c]*Laboratoire Physico-chimie des Electrolytes, Colloïdes et Sciences Analytiques (PECSA), UMR 7195 CNRS, Université Pierre et Marie Curie, Paris, France*
† Electronic supplementary information (ESI) available. See DOI: 10.1039/c1lc20263d

aqueous gel that are cast onto substrates composed of an array of micro-holes. We thus fabricated arrays of magnetic micropillars. Then, by using an external magnetic field, we were able to locally and/or globally induce the deformation of the micropillars. In particular, we achieved for the first time the simultaneous actuation of a large number of adjacent micropillars.

Experimental

Micropillar substrate generation

Microfabrication methods for arrays of micrometre sized pillars have been previously described.[15] We used PAM hydrogels to replicate mold arrays of pillars from silicon-etched wafers. PAM gels were prepared by mixing acrylamide and its crosslinker bis-acrylamide in various proportions, allowing access to a certain range of rigidity.[16,17] We used concentrations of acrylamide (10% to 20% v/v) and bis-acrylamide (0.5% to 1% v/v) which give rigidities from 100 to 250 kPa. The reticulation of PAM was chemically induced by adding initiators such as ammonium persulfate (Bio-Rad) and TEMED (Bio-Rad). Then a small droplet (around 50 μL) was deposited on a micropatterned silicon wafer. The PAM gels took around 1 hour to reticulate. As PAM hydrogels did not reticulate in the presence of oxygen, we used glass coverslips to seal the gel during the curing process. Coverslips were previously treated with a mixture of 1/7 ethyl alcohol, 3/7 bind silane (Amersham Biosciences) and 3/7 acetic acid (VWR) for 20 minutes. This process enabled the PAM gel to adhere on the coverslip and facilitate the peeling process off the wafer in water. Finally we obtained a substrate made of an array of PAM micro-pillars.[18]

Preparation of magnetic nanoparticles

We used two different kinds of particles. We first tried ferromagnetic black iron oxide particles of 200 nm diameter (Polysciences) up to a concentration of 5% (w/w). These particles were directly mixed with the acrylamide–bis solution which was then sonicated for 15 minutes to avoid aggregates formation. Then the unreticulated mixture was poured onto the wafer and we gently centrifugated it (1 min at 4000 rpm) to force particles accumulation into the holes etched at the surface of the wafer. We also used specifically designed superparamagnetic colloids made by controlled aggregation of negatively charged maghemite nanoparticles and cationic-neutral diblock copolymer.[19] In this case, iron oxide nanoparticles (bulk mass density = 5100 kg m^{-3}) were synthesized according to the Massart technique by alkaline co-precipitation of iron (II) and iron(III) salts, oxidation of the magnetite (Fe_3O_4) into maghemite (γ-Fe_2O_3) nanoparticles, and by size-sorting by subsequent phase separations. The ferrofluid dispersions were characterized by electron microdiffraction, vibrating sample magnetometry, magnetic sedimentation and light scattering. The size distribution of the magnetic nanoparticles was determined from transmission electron microscopy (TEM) measurements, as previously described.[19] We obtained an average diameter of 7 nm. The particles were then functionalized with poly(acrylic acid) chains, a procedure which allowed to reverse the surface charges from cationic at low pH to anionic at high pH through the ionization of the carboxyl groups. In a second step, the particles were assembled using electrostatic interactions to build large supracolloidal aggregates. The co-assembly process was done with poly(trimethylammonium ethylacrylate)-*b*-poly(acrylamide) ($PTEA_{11K}$-*b*-PAM_{30K}) as a copolymer (molecular weights of 11 000 g mol^{-1} and 30 000 g mol^{-1}) and leads to aggregates with a 20 nm thick PAM corona insuring an excellent compatibilization with the PAM hydrogel matrix. The aggregates formed were either spherical clusters of diameter 200–500 nm or elongated nanowires of diameter 200 nm and length 5–15 μm. The mixture was sonicated for 15 minutes and degassed under vacuum in order to remove oxygen. Finally, to increase the concentration in magnetic particles inside the pillars we used a magnetic field. As the magnetic particles had the tendency to aggregate along the magnetic field lines, we used two magnets and put the wafer closer to one of the magnets so that the clusters and rods were aligned with the pillar direction and were attracted into them at the same time (Fig. 1A).

Magnetic field generation

As the force applied on magnetic particles depends both on the amplitude and the gradient of the magnetic field ($F = (m\nabla)B$) an easy way to achieve high forces is to use a sharp magnetized tip.[20] The magnet microneedle which consists of a stainless steel needle attached to a permanent magnet (rare earth magnet, Radiospares, France) was mounted on a micromanipulator (Sutter Instruments, MP 285). Hence by focusing the magnetic field lines, a strong gradient was created at its extremity. To calibrate the magnetic field gradient, we used calibrated magnetic beads that were subjected to the force induced by the magnetized needle in a solution with well-defined viscosity.[20] The particle was subjected to a force proportional to the local field gradient $F = (m\nabla)B$ where m is the magnetic moment of the particle. The spherical particle was also subjected to viscous force according to the

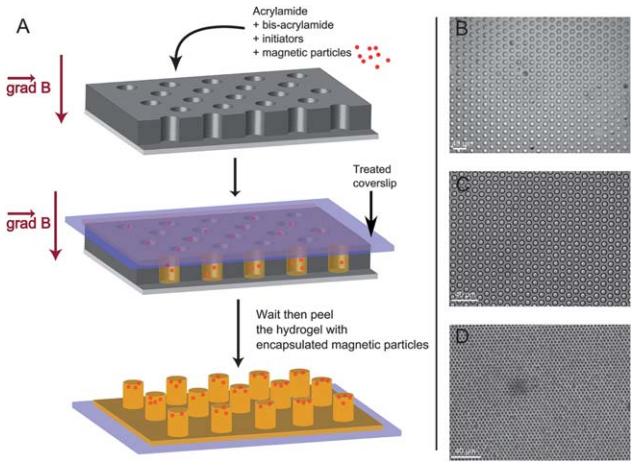

Fig. 1 (A) Schematic illustration of the different steps for preparing magnetic micropillar substrates. The acrylamide–bisacrylamide solution is mixed with the magnetic particles and poured on the silicon wafer previously cleaned with an air plasma cleaner for 30 s. Two permanent magnets are used to increase the concentration in magnetic particles inside the micro-structures. When peeled off, we obtain large arrays of micro-pillars of different sizes. (B) An array of pillars of 10 μm diameter and 20 μm height. (C) An array of pillars of 5 μm diameter and 15 μm height. (D) An array of pillars of 2 μm diameter and 6 μm height.

Stokes' law. Knowing the saturated magnetic moment of the particles, we could thus evaluate the magnetic force as well as the magnetic field gradient (see ESI, Fig. S1†). We found gradient values up to 230 ± 20 G μm^{-1} at a distance, D, between the tip of the needle and the pillar of around 10 μm.

Measurements of forces and substrate deformations

The micropillar substrates were examined by optical microscopy using an inverted microscope (Olympus, IX71). The deformation of the pillars was measured using both a particle analysis plugin and a tracking plugin (ImageJ software). The gel rigidity was independently measured using a macroscopic cylindrical sample of the gel and a bench of compression (Stable Micro Systems) which allowed to exert a controlled stress on the sample and to measure its deformation at the same time.

Results and discussion

Fabrication principle of micropillar substrates with embedded magnetic nanoparticles

Shown in Fig. 1A is a schematic illustration of the procedure used to obtain magnetic micropillars through a replica molding technique.[15,18] PAM gels mixed with magnetic particles were poured and polymerized on a silicon wafer that contained microfabricated cylindrical holes. The dimensions of these holes were varied from 5–20 μm in depth and from 3–20 μm in diameter. Hence this technique enabled the fabrication of PAM micropillar substrates with various dimensions over large areas (about 1 cm^2) as shown in Fig. 1B–D. We developed different strategies to disperse magnetic particles such as black iron oxide particles and ferrofluids[19] as well as magnetite nanoparticle complexes.[14,19]

The aggregation of such particles inside PDMS matrices made the insertion of magnetic particles inside microstructures difficult. In contrast, using PAM gels improved the dispersion of the particles within the matrix. Besides improving dispersion, the use of PAM gels ensures the suitability of the device for biological application: such gels are commonly used to study cell adhesion and migration on flat substrates.[21] Finally, the stiffness of PAM gels can be easily controlled by changing the proportion of bis/acrylamide.[16] Here, we varied the rigidity of the substrate, E, from 100 kPa up to 250 kPa. By doing so, we obtained micropillar substrates with well-suited mechanical properties. The dimensions of the pillars and the Young's modulus, E, of the gel control the effective rigidity of the pillar. To a first approximation, the elastic force, F, associated with pillar deformation is given by the following formula (eqn (1)):

$$F = K\Delta x = \frac{3}{4}\pi E\frac{r^4}{L^3}\Delta x \quad (1)$$

where k, Δx, r and L are the spring constant, the deflection, the radius and the height of the pillars, respectively. Thus we obtained a range of spring constants varying from 0.2 up to 400 nN μm^{-1}.

Synchronized movements of magnetic micropillars

First, we reproducibly managed to fabricate large areas of homogeneous magnetic micropillars whose diameter was larger than 10 μm by incorporating basic ferromagnetic black iron oxide particles with an average size of around 200 nm. The application of a magnetic field during gel reticulation enabled the optimization of the incorporation of magnetic particles inside the micro-pillars (Fig. 1A). As shown in Fig. 2B and C, this procedure allowed to concentrate the nanoparticles inside the pillars since the bottom substrate appeared transparent to light and the pillar areas opaque. Interestingly, a side view of the pillars (Fig. 2B) showed that the nanoparticles were indeed concentrated at the top of the pillars. After reticulation, the application of a magnetic field gradient leads to a global displacement of the pillars in the vicinity of the needle (Fig. 2 and Movie S1†). Shown in Fig. 2C is an example of a PAM gel ($E \approx$ 210 kPa) composed of magnetic micropillars whose height and diameter were 20 and 10 μm, respectively. We observed an average displacement of around 5 μm. Importantly, our experiments showed that it was indeed possible to force the movement of a large number of pillars in a synchronous way (Fig. 2C). Magnetic pillars could be forced to adopt precessive movements as they followed the position of the magnetic tip (Fig. 2D) and thus be oriented in any direction. The magnetically activated area depended on the magnetic field generated at the tip of the magnetic needle, but could typically extend over 5–10 pillars. Our method allowed us to impose a time varying motion of several pillars. As the magnetic force was proportional to the field gradient, the amplitude of displacements decreased with the distance, D, from the tip of the needle. We observed a maximal displacement of the micropillars of 6 μm (Fig. 2D and see ESI, Fig. S2†). Using this method, we obtained around 60% of the micropillars doped with the magnetic material in the central part of the substrate where the magnetic field was applied.

Alternatively, we used specifically designed super-paramagnetic aggregates fabricated by the co-assembly of ferrofluid suspensions and block copolymers exhibiting PAM at their surface[19,22] and thus facilitating the dispersion of the aggregates into PAM gels (Fig. 3A and 5B).

Another advantage of using such super-paramagnetic aggregates is the possibility to control the shape of the nanoparticles to obtain either spherical aggregates with an average diameter of around 250 nm or polydisperse nanowires with a typical maximal length of typically 10 μm.[19] We used the same procedure as described previously to fabricate magnetic PAM micropillars with these PAM compatible particles (see Material and methods section). With such particles, we did not observe the formation of aggregates when mixed with PAM gels with neither types of particles (spherical or nanowires). Importantly, we managed to incorporate these magnetic nanoparticles into smaller micropillars down to a diameter of 3 μm.

With a high concentration of spherical aggregates, we made arrays of micropillars which were, similarly to the case of basic ferromagnetic particles, collectively actuable by a magnetic field gradient (Fig. 3B and Movie S2†). Again large areas of micropillars showed a reliable actuation under the magnetic field gradient, even those whose diameter was smaller than in the previous case (ϕ = 5 μm instead of 10 μm). For example, Fig. 3B shows the synchronized movement of pillars imposed by the movement of the magnetic needle in its vicinity leading to an average deflexion of around 1 μm. The deformation of the pillars was localized near the magnetic tip of the needle where an intense field gradient was generated.

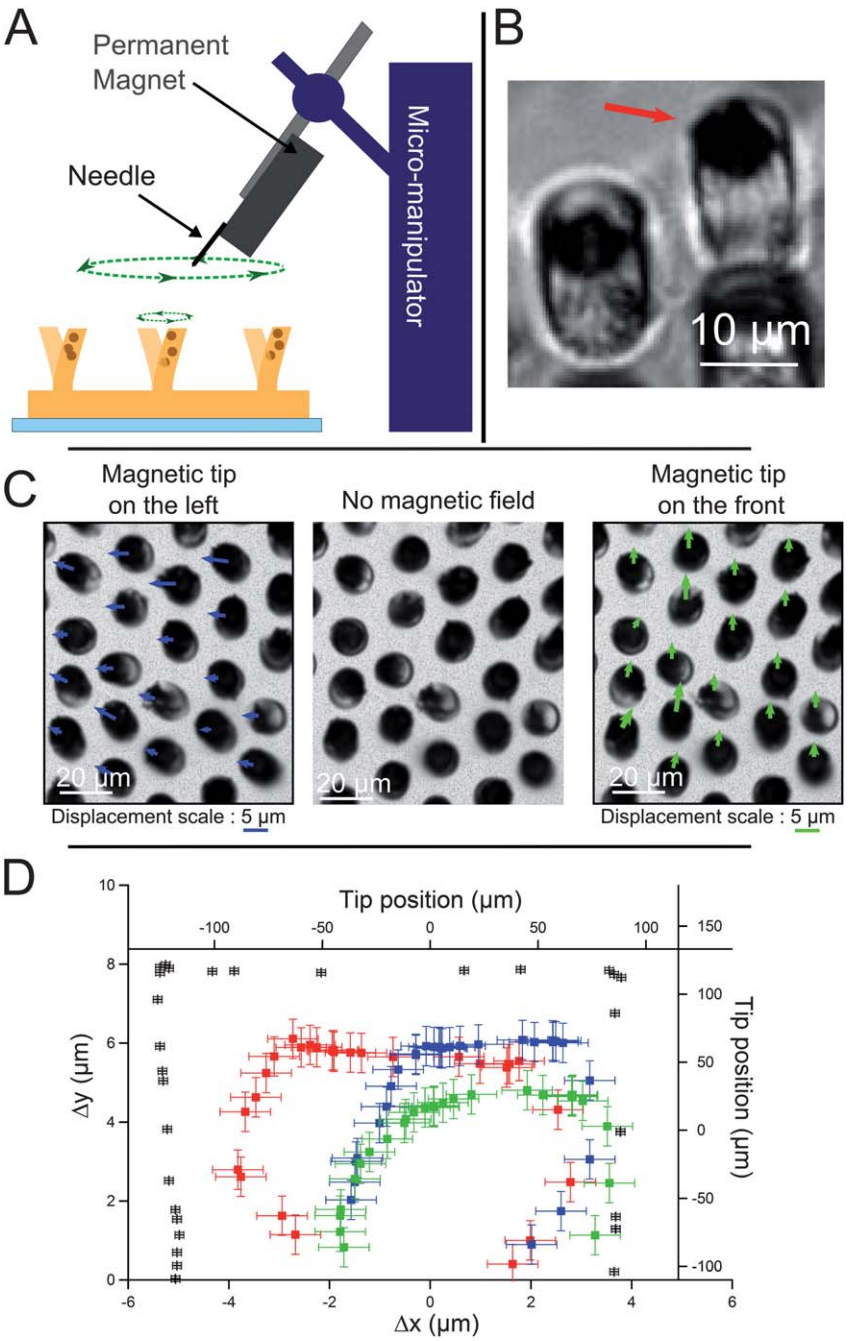

Fig. 2 (A) Schematic illustration of the experimental setup used to create magnetic field gradients. A sharp metallic needle was mounted on a piezo-electric micromanipulator. Using spherical magnetic aggregates, it is possible to obtain a large array of magnetic micro-pillars. The substrate is thus homogeneously deformed when a strong magnetic field gradient is applied. A home-made analysis software enables to detect the position of each pillar. It appears that each pillar followed the movement of the magnetic tip. (B) Side view of pillars with a 10 µm diameter and 20 µm height filled with ferromagnetic black iron oxide particles. Using our technique, magnetic nanoparticles are concentrated at the top of the pillars. (C) A first example shows optical images of the movement of those pillars. The movement of the needle induced a rotation motion of the pillar (left and right pictures). (D) Displacements of 3 independent pillars. The deformation follows the motion of the magnetic tip except for large angles because in such a case the magnetic force is not only due to the gradient at the tip of the needle but is distributed along the needle.

To estimate the magnetic force exerted on the micropillars, we measured the deflection of a pillar relatively to its distance to the magnetic needle tip (Fig. 4). Fig. 4B shows the displacements of micropillars of similar dimensions ($\phi = 5$ µm; $L = 15$ µm) but with two different Young's moduli (120 and 240 kPa) under a magnetic gradient. As expected, we observed that the deflection strongly decreased with the distance, D, to the magnetic tip. For $D > 80$ µm, we could not detect any significant deflection. For softer gels (~120 kPa), we moreover verified that the magnetic field gradient induced larger deformations than for stiffer gels (~240 kPa).

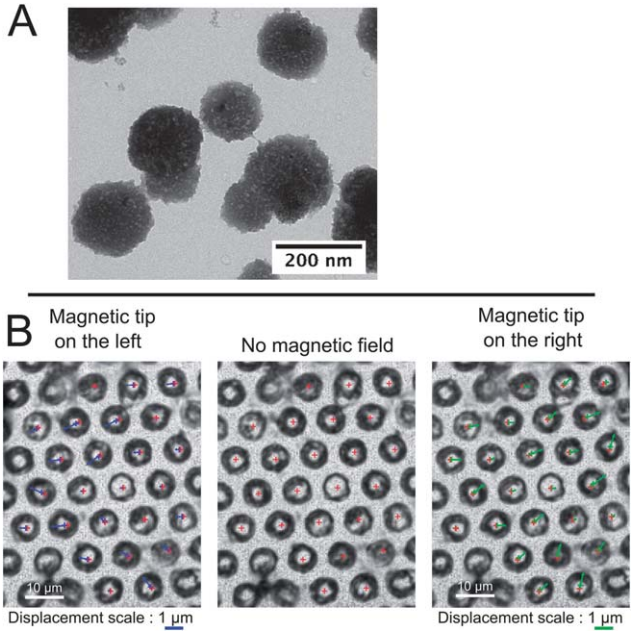

Fig. 3 (A) TEM image of magnetic spherical aggregates obtained by the electrostatic co-assembly of iron oxide nanoparticles and polymers. (B) Example showing the coordinated movement of pillars of 5 µm diameter and 15 µm height with two positions of the magnetic tip.

Assuming that the restoring elastic force was given by eqn (1), we computed the force induced by the deformation of the pillar (Fig. 4C). Interestingly, we found for both rigidities the same force curves as a function of D. This shows that the magnetic properties of pillar substrates with embedded magnetic nanoparticles did not depend on the chemistry of the gel but rather on the geometrical properties of the pillars and that it could be reproducibly adjusted. Using spherical magnetic nanoparticles, we showed that we could fabricate magnetic pillars with a diameter as small as 4 µm. Such small pillars could be particularly useful to study cell mechanics and cell response to external forces. In such a case, we estimated the magnetic force exerted on a micropillar and compared it to the elastic force. To do so, we prepared micropillar substrates with a height of 14 µm by mixing the PAM solution with the nanoparticles up to a final concentration of maghemite of around 6.3 mM. By applying the maximum field gradient on the pillars, we induced a maximal deformation of the pillars of around 0.25 µm. It corresponded to an elastic force of around 490 pN according to eqn (1) (Fig. 4C). Knowing the saturation magnetization of maghemite $J_s \approx 80$ A m^2 kg^{-1}, we evaluated the magnetic force exerted on one pillar. At nearly 10 µm from the magnetic tip, the magnetic field gradient was around 23×10^3 T m^{-1}. An estimation of the magnetic force could thus be given by the following formula (eqn (2)):

$$F \approx J_s m_{\text{maghemite}} |\nabla B| \quad (2)$$

where $m_{\text{maghemite}}$ was the mass of maghemite included in one pillar. We obtained a maximum force of around 370 pN, which was consistent with the estimation of the spring force.

Altogether, our findings demonstrated that we could induce a global motion of pillars in the vicinity of the magnetized needle in a reproducible and well-defined manner.

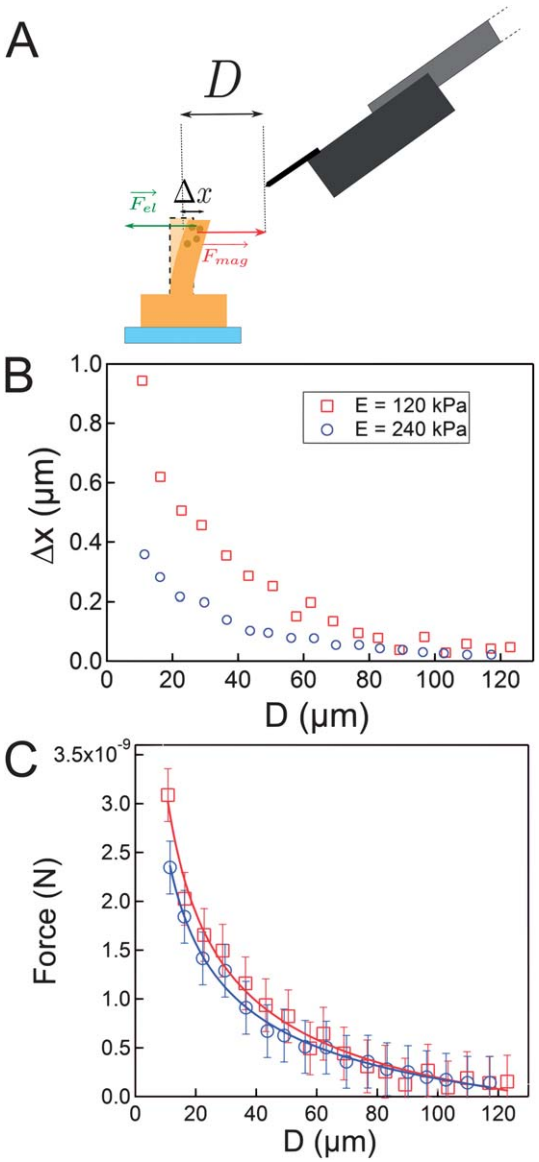

Fig. 4 (A) Schematic representation of the forces exerted on a magnetic pillar: a magnetic force induced by the field gradient and the restoring elastic force. Δx is the displacement of the pillar, D its distance to the magnetic tip. (B) Experimental data of the displacement of pillars as a function of their distance from the tip of the needle for two different rigidities, 120 and 240 kPa represented by □ (in red) and ○ (in blue) respectively (12% acrylamide/0.6% bis for 120 kPa and 19% acrylamide/0.9% bis for 240 kPa). Using pillars with a diameter of 5 µm and a height of 15 µm, we observed a rapid decrease in the displacement as a function of D for both rigidities. (C) Force curves as a function of D. The forces were calculated from the experimental data of the displacements according to eqn (1). We obtained the same force curves within the error bars, confirming that the incorporation of magnetic particles did not depend on the chemistry of PAM gels.

Local dynamics of magnetic pillars using magnetic nanowires

As previously mentioned, we could also use magnetic nanowires instead of spherical aggregates (Fig. 5B). In this case, by decreasing the concentration of nanowires inside the PAM gel (Fig. 5A) and using the same procedure for the fabrication of

micropillar substrates, we could fabricate substrates with only a few magnetic pillars, randomly placed and surrounded by many nonmagnetic ones (Fig. 5C and Movie S3†). We used pillars with a diameter of 5 μm, a height of 15 μm and a Young modulus $E = 160$ kPa which corresponded to a spring constant of around 3 nN μm^{-1}. With such strategy we obtained a local movement of the pillars with a displacement of around 3 μm, corresponding to forces in the nanoNewton range. Indeed, using eqn (2) and a volume fraction of magnetic material inside a nanorod[19,22] of 0.2, it is possible to calculate the force exerted by the magnetic gradient on one nanorod. The insertion of nanowires with a diameter of 250 nm and a length of 15 μm enables to reach forces of around 4 nN, which is consistent with the evaluation of the spring force. Let us notice that such forces are on the range of what eukaryotic cells are exerting and are enough to deform the cell cortex.[5]

A recent study by Sniadecki *et al.*[23] showed that super-paramagnetic nanowires could be incorporated into PDMS micropillars to induce only a local movement of isolated pillars. However, this technique was based on the bending of the pillar with a homogeneous magnetic field instead of the magnetic field gradient. As the direction of the magnetic moment was set by the external field, the bending direction of the pillar did not change when the magnetic field was reversed. In contrast, we confirmed here that a magnetic field gradient induced a displacement of the pillar in any direction (Fig. 5C and Movie S3†).

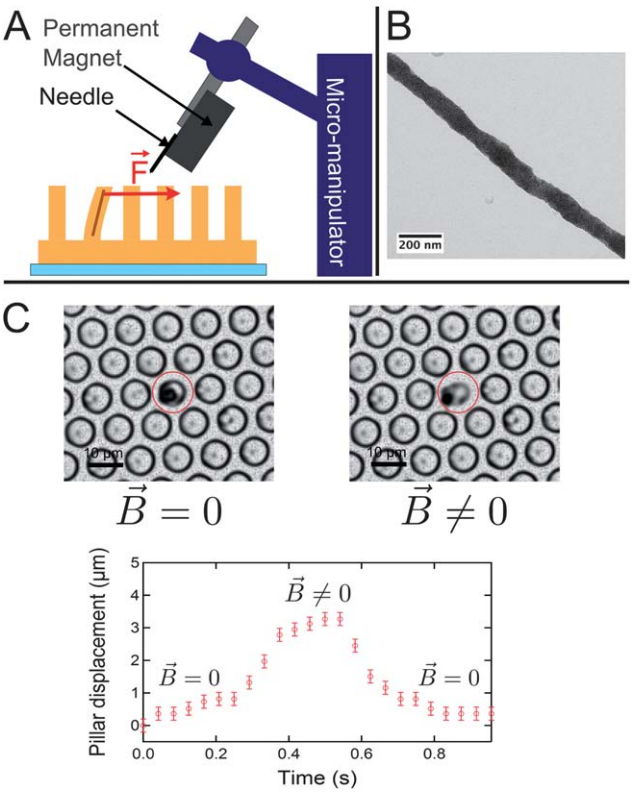

Fig. 5 (A) Schematic representation of the forces exerted on a magnetic pillar made with magnetic nanowires. The use of magnetic nanowires enabled to locally deform the substrate. (B) TEM image of a magnetic nanorod. (C) Only one localized pillar was magnetized and deformed while a magnetic field gradient was applied. Pillars have a diameter of 5 μm and a height of 15 μm. The graph represents the pillar displacement when the magnetic field is either turned on or off as a function of time.

Concluding remarks

We have introduced a new and versatile method to induce the actuation of microfabricated substrates, which involves the fabrication of magnetic micropillars. Based on different approaches, we have demonstrated that we could induce a global or local actuation of the substrates. Pillars move collectively in a synchronous way when prepared with a high density of magnetic particles whereas a few magnetic pillars can be interspersed among nonmagnetic ones by using a low density of nanowires. Our method could be used to exert static and dynamical forces on the basal side of living cells or to induce cell alignment and/or tissue patterning.

Acknowledgements

We thank A. Buguin, P. Silberzan, P. Keller and J. Malthête for helpful discussions. This work was supported by the Agence Nationale de la Recherche (ANR) (Programme PNANO 2005 & Programme Blanc 2010 SVSE5 "MECANOCAD"), the C'nano Ile de France, Ligue Nationale contre le Cancer (Comité Ile-de-France), Association Française contre les Myopathies and the CNRS (Program Prise de Risques "Interface physique, biologie et chimie"). This research is also supported in part by Rhodia (France), by the ANR under the contract BLAN07-3_206866, by the European Community through the project: "NANO3T—Biofunctionalized Metal and Magnetic Nanoparticles for Targeted Tumor Therapy", project number 214137 (FP7-NMP-2007-SMALL-1) and by the Région Ile-de-France in the DIM framework related to Health, Environment and Toxicology (SEnT).

References

1 Y. N. Xia and G. M. Whitesides, *Annu. Rev. Mater. Sci.*, 1998, **28**, 153–184.
2 N. Pamme, *Lab Chip*, 2006, **6**, 24–38.
3 F. Fahrni, M. W. J. Prins and L. J. van Ijzendoorn, *J. Magn. Magn. Mater.*, 2009, **321**, 1843–1850.
4 C. S. Chen, J. Tan and J. Tien, *Annu. Rev. Biomed. Eng.*, 2004, **6**, 275–302.
5 D. A. Fletcher and D. Mullins, *Nature*, 2010, **463**, 485–492.
6 D. Quere and M. Reyssat, *Philos. Trans. R. Soc., A*, 2008, **366**, 1539–1556.
7 J. le Digabel, M. Ghibaudo, L. Trichet, A. Richert and B. Ladoux, *Med. Biol. Eng. Comput.*, 2010, **48**, 965–976.
8 J. L. Tan, J. Tien, D. M. Pirone, D. S. Gray, K. Bhadriraju and C. S. Chen, *Proc. Natl. Acad. Sci. U. S. A.*, 2003, **100**, 1484–1489.
9 I. Schoen, W. Hu, E. Klotzsch and V. Vogel, *Nano Lett.*, 2010, **10**, 1823–1830.
10 R. G. Flemming, C. J. Murphy, G. A. Abrams, S. L. Goodman and P. F. Nealey, *Biomaterials*, 1999, **20**, 573–588.
11 M. T. Frey, I. Y. Tsai, T. P. Russell, S. K. Hanks and Y. L. Wang, *Biophys. J.*, 2006, **90**, 3774–3782.
12 W. Roos, J. Ulmer, S. Grater, T. Surrey and J. P. Spatz, *Nano Lett.*, 2005, **5**, 2630–2634.
13 F. Pirmoradi, L. N. Cheng and M. Chiao, *J. Micromech. Microeng.*, 2010, **20**, 015032.
14 K. S. Wilson, J. D. Goff, J. S. Riffle, L. A. Harris and T. G. St Pierre, *Polym. Adv. Technol.*, 2005, **16**, 200–211.
15 M. Ghibaudo, J. M. Di Meglio, P. Hersen and B. Ladoux, *Lab Chip*, 2011, **11**, 805–812.

16 R. J. Pelham and Y. L. Wang, *Proc. Natl. Acad. Sci. U. S. A.*, 1997, **94**, 13661–13665.
17 C. E. Kandow, P. C. Georges, P. A. Janmey and K. A. Beningo, in *Methods in Cell Biology*, Academic Press, 2007, vol. 83, pp. 29–46.
18 N. Biais, B. Ladoux, D. Higashi, M. So and M. Sheetz, *PLoS Biol.*, 2008, **6**, e87.
19 J. Fresnais, J. F. Berret, B. Frka-Petesic, O. Sandre and R. Perzynski, *Adv. Mater.*, 2008, **20**, 3877–3881.
20 M. Tanase, N. Biais and M. Sheetz, in *Cell Mechanics*, Elsevier Academic Press Inc, San Diego, 2007, vol. 83, pp. 473–493.
21 D. E. Discher, P. Janmey and Y. L. Wang, *Science*, 2005, **310**, 1139–1143.
22 J. Fresnais, C. Lavelle and J. F. Berret, *J. Phys. Chem. C*, 2009, **113**, 16371–16379.
23 N. J. Sniadecki, A. Anguelouch, M. T. Yang, C. M. Lamb, Z. Liu, S. B. Kirschner, Y. Liu, D. H. Reich and C. S. Chen, *Proc. Natl. Acad. Sci. U. S. A.*, 2007, **104**, 14553–14558.

